Tip Leakage Flow in Axial Compressors

J. A. Storer

N. A. Cumpsty

Whittle Laboratory,
University of Cambridge,
Cambridge, United Kingdom

Experimental measurements in a linear cascade with tip clearance are complemented by numerical solutions of the three-dimensional Navier–Stokes equations in an investigation of tip leakage flow. Measurements reveal that the clearance flow, which separates near the entry of the tip gap, remains unattached for the majority of the blade chord when the tip clearance is similar to that typical of a machine. The numerical predictions of leakage flow rate agree very well with measurements, and detailed comparisons show that the mechanism of tip leakage is primarily inviscid. It is demonstrated by simple calculation that it is the static pressure field near the end of the blade that controls chordwise distribution of the flow across the tip. Although the presence of a vortex caused by the roll-up of the leakage flow may affect the local pressure field, the overall magnitude of the tip leakage flow remains strongly related to the aerodynamic loading of the blades.

Introduction

Large tip clearance is recognized to be detrimental to both the efficiency and stability of axial compressors (Smith, 1970; Freeman, 1985). In most cases optimum performance is obtained at a clearance smaller than that dictated by mechanical constraints. Deliberate aerodynamic design to minimize the deleterious effects of tip leakage therefore remains the only option for further improvement, but such design cannot be fully effective without an appreciation of the factors governing tip leakage flow.

The work described in this paper is an investigation of tip leakage flow in a linear cascade using a combination of experimental measurements and three-dimensional numerical solutions of the Navier–Stokes equations. The calculations are used to explore aspects of tip leakage flow less accessible by experiment alone. Although the flowfield near the endwalls of a linear cascade is known to differ considerably from that in a compressor, this difference is of secondary importance to the present investigation because attention is directed to the leakage flow itself.

Experimental Methods

All the experimental results described in this paper were obtained in a linear cascade comprising five blades. Details of the aerodynamic design of the cascade are given in Table 1. The central blade was instrumented with pressure tappings on both surfaces at several spanwise positions near the tip. The blades were cantilevered so they could be moved relative to the endwalls to vary the clearance gap at the tip by adjusting the hub fixture.

The periodicity of the flow was controlled by adjustable flaps at the top and bottom of the cascade. This arrangement was adequate since it was only necessary to achieve the design flow conditions about the central aerofoil, around which the leakage flow measurements were to be taken. Comparison of the pressure distribution measured at midspan with a prediction by an inviscid (Martensen) calculation confirms the cascade was set up correctly (see Fig. 1).

Table 1 Summary of cascade aerodynamics

Chord	300.0 mm
Pitch	180.0 mm
Span	435.0 mm
Maximum thickness-to-chord ratio	0.05
Camber (circular arc)	45.5°
Stagger	22.2°
Inlet flow angle from axial	45.0°
Inlet Mach number	0.03
Reynolds' number based on chord	5.0×10^5
Inlet endwall boundary layer 140% chord upstream:	
Displacement thickness	2.9 mm
Momentum thickness	2.1 mm
Shape factor	1.4

Measurements of the static pressure on the endwall were made with a matrix of pressure tappings drilled in the endwall to span the two blade passages about the central blade. The distribution of pressure tappings on the endwall was nonuniform and reflected the anticipated pressure gradients. In total 522 tappings were arranged in a square mesh with the smallest spacing between adjacent tappings being 3 mm (1 percent of chord). The measurements were taken in blocks of 48 connected via a Scanivalve to a single pressure transducer.

Detailed measurements of the leakage flow were carried out at fixed positions along the blade chord for a variety of clearances. Traverses were made across the tip gap to an accuracy

Contributed by the International Gas Turbine Institute and presented at the 35th International Gas Turbine and Aeroengine Congress and Exposition, Brussels, Belgium, June 11–14, 1990. Manuscript received by the International Gas Turbine Institute February 10, 1990. Paper No. 90-GT-127.

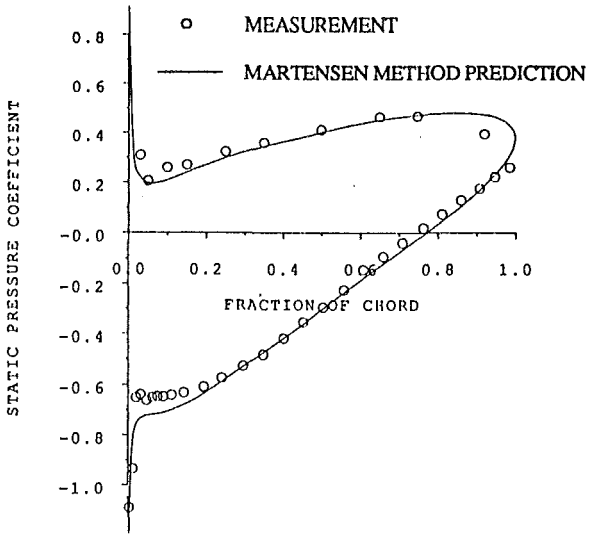

Fig. 1 Blade pressure distribution at midspan

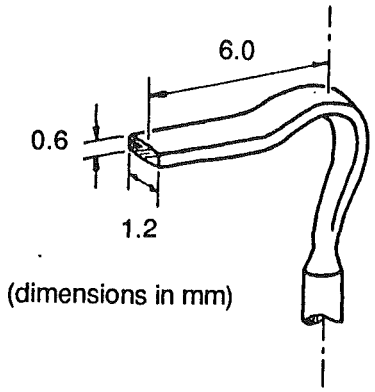

Fig. 2 External dimensions of pressure probe

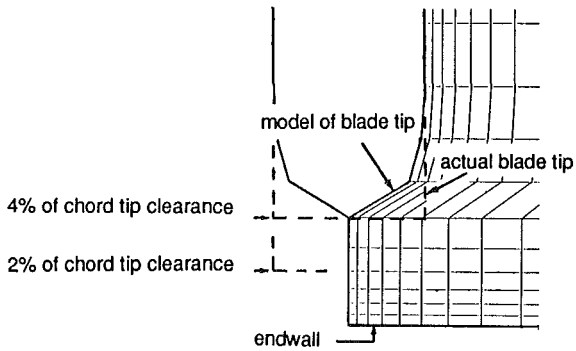

Fig. 3 Typical computation mesh at blade tip

in space of ±0.03 mm (±1 percent of the smallest clearance examined). Measurements were only made of the flow leaving the tip gap on the suction side of the blade where it was assumed the flow would be nearly parallel to the endwall and the static pressure would be effectively uniform across the height of the clearance gap. A flattened Pitot probe and a two-hole probe of the same external dimensions were used to give information on total pressure, flow speed, and direction. The size of the probes is indicated in Fig. 2. The combination of probes was equivalent to a single three-hole probe but was used in preference so as to keep probe blockage to a minimum and to improve the resolution of the measurements. The flow speed at the blade tip was obtained from a calibration of the two-hole probe assuming incompressible flow and has been nondimensionalized by the inlet velocity to the cascade. Flow direction was measured to ±0.5 deg by adjusting the yaw of the two-hole probe. Flow angles are quoted with reference to the notional axial direction of the cascade (the normal to the plane containing the leading edges).

All pressures were measured relative to the free-stream total pressure ahead of the cascade and were recorded automatically by a data logging system to an accuracy of within ±0.3 percent of the reading. The measurements of pressure are presented in two ways: static pressures are quoted as a static pressure coefficient, C_P, defined as

$$C_P = \frac{(p - p_1)}{(P_{01} - p_1)} \tag{1}$$

while total pressures are given as total pressure loss coefficient, ω, where

$$\omega = \frac{(P_{01} - P_0)}{(P_{01} - p_1)} \tag{2}$$

The inlet velocity was measured by a Pitot-static probe in the free stream ahead of the cascade and was maintained at 24 m/s giving an inlet Mach number to the cascade of 0.03.

Numerical Analysis Technique

Solutions of the three-dimensional Navier–Stokes equations for the flow in the cascade were obtained from the finite volume method of Dawes (1987). Closure is obtained in this code with a mixing length turbulence model patterned after Baldwin and Lomax (1978). The code is fully vectorized and executes on a single processor of an Alliant FX/8 computer at approximately 5×10^{-3} seconds per point per time step. Typically about 1500 time steps were needed for acceptible convergence on a $33 \times 61 \times 25$ mesh.

The code calculates tip leakage flow but does not attempt faithfully to model the conditions in the tip gap. Instead the computation mesh is rounded to a single point at the blade tip, above which a normal periodic boundary is assumed. An enlargement of the typical mesh around the blade tip with 4 percent clearance is shown in Fig. 3. The computation scheme is unsuited to flow of very low Mach number and it was necessary to assume an inlet Mach number of 0.3 for the present calculations. This value is sufficiently subsonic for the steady solution to resemble incompressible flow. The correct blade Reynolds number of 5.0×10^5 was maintained.

Results

Pressure on the Endwall. Static pressure on the endwall was measured with the tip clearance set to zero, 2 percent, and

Nomenclature

C_D = discharge coefficient (actual flow ÷ ideal flow rate)
C_P = static pressure coefficient = $(p - p_1)/1/2\rho V_1^2$
C_F = tangential blade force coefficient = $F_T/1/2\rho s V_x^2$
F_T = tangential blade force
p = static pressure
P_0 = total pressure
Re_C = Reynolds number based on blade chord
Re_δ = Reynolds number based on tip gap height
V = velocity
$\bar{V}$ = area mean velocity
ρ = density
ω = total pressure loss coefficient = $(P_{01} - P_0)/1/2\rho V_1^2$

Subscripts

0 = stagnation value
1 = reference in free stream ahead of cascade
L = in leakage direction
loc = local
p = pressure side
s = suction side
S = in streamwise direction

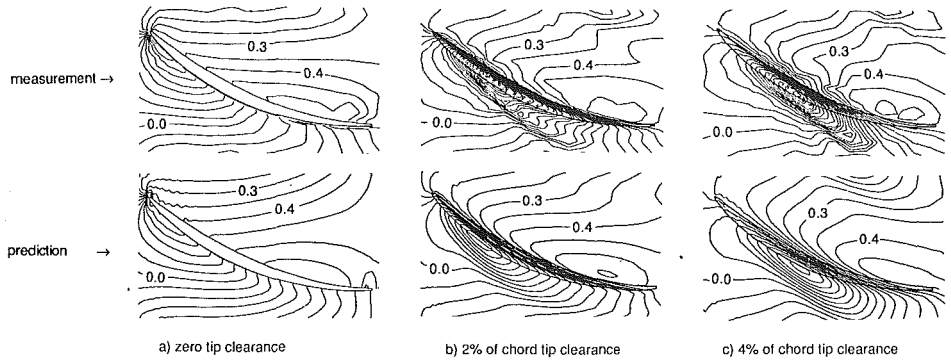

Fig. 4 Measured and predicted endwall static pressure distributions

4 percent of chord (clearances representative of those that can occur in a multistage machine). Contours of pressure measured on the endwall are shown in the upper part of Fig. 4; pressures calculated with the Navier–Stokes code are shown in the lower portion of the same figure for direct comparison. A contour interval of 5 percent inlet dynamic head is used throughout. The agreement between measurement and the prediction is very good.

With both 2 percent and 4 percent of chord tip clearance, visualization of the flow on the endwall by oil marked with fluorescent powder and tests with a wool tuft revealed the presence of a vortex in the passage near the blade tip. The trajectory of the vortex coincided with a trough of pressure measured on the endwall; a similar trough is evident in the numerical solution. The origin of the trough is close to the lowest pressure contour on the endwall, which is located close to the blade tip. The position of minimum pressure on the endwall moves progressively downstream of the leading edge as the tip clearance is increased. With 2 percent clearance the minimum pressure is located about 25 percent of chord from the leading edge; with 4 percent clearance it is near 42 percent of chord (see Fig. 4). The Navier–Stokes calculation predicts this change and is able to establish the correct location of the minimum pressure contour.

Blade Surface Pressure Distribution. Measurements were also made of the static pressures on the blade surfaces with tip clearances of zero, 2 percent, and 4 percent of chord.

With zero tip clearance the loading near the end of the blade was less than that near midspan (see Fig. 5). A contour plot of measured pressure on the suction surface without tip clearance (Fig. 6) reveals lines of constant pressure to be curved forward as a result of the blockage from the corner separation formed to the rear. This gives rise to a spanwise pressure gradient with generally higher pressure toward the tip, especially close to the leading edge. In spite of this the loading of the blade remains relatively high near the leading edge and resembles that at midspan.

When there is tip clearance, the pressure distribution near the tip may change significantly from that near midspan. The pressure distribution measured near the tip with 4 percent clearance is shown in Fig. 7, where it is compared with the distribution at midspan. In general tip clearance causes the pressure on the pressure side to be lower near the tip, especially near the leading edge. On the suction side the pressure near the tip tends to be higher near the leading edge. Toward the trailing edge a beneficial interaction of the tip leakage flow with the endwall flowfield prevents the corner separation found without tip clearance and locally the pressure on the suction side becomes similar to that at midspan. Near midchord, however, the pressure on the suction side tends to be reduced by the tip leakage vortex as discussed below.

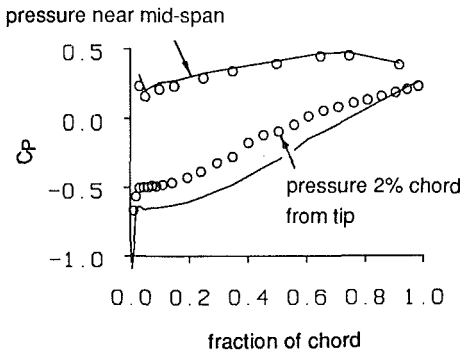

Fig. 5 Blade pressure distribution with zero tip clearance

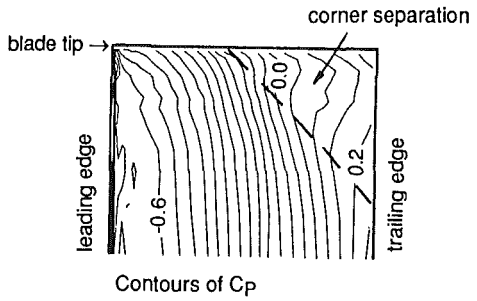

Fig. 6 Suction surface pressure distribution with zero clearance

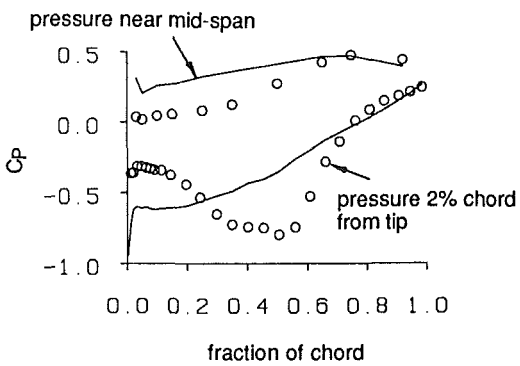

Fig. 7 Blade pressure distribution with 4 percent of chord tip clearance

Flow at Exit of Tip Gap. Detailed measurements of the leakage flow leaving the tip gap were made with the gap set to both 2 percent and 4 percent of chord. Measurements were made at 25 points across the gap at 10 chordwise locations. In general the pattern of the leakage flow was similar at both clearances and, to aid presentation, the salient features have been summarized by a selection of the measurements made at 4 percent clearance in Fig. 8. Shown in the figure are the

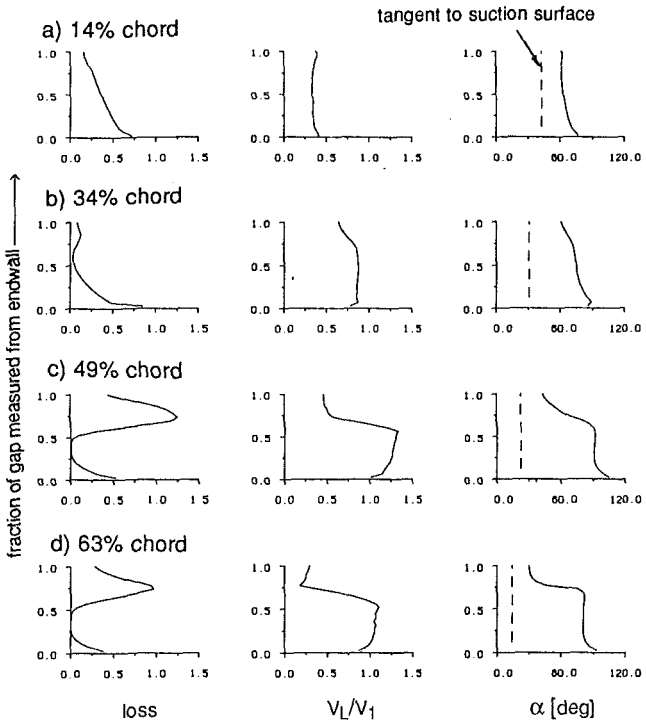

Fig. 8 Measurements of the flow leaving the tip gap on the suction side with 4 percent chord tip clearance

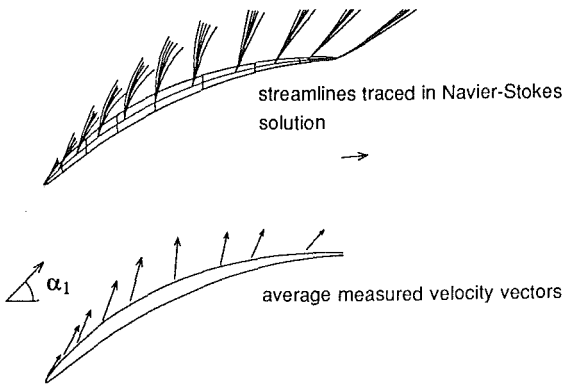

Fig. 9 Leakage flow direction with 4 percent of chord tip clearance

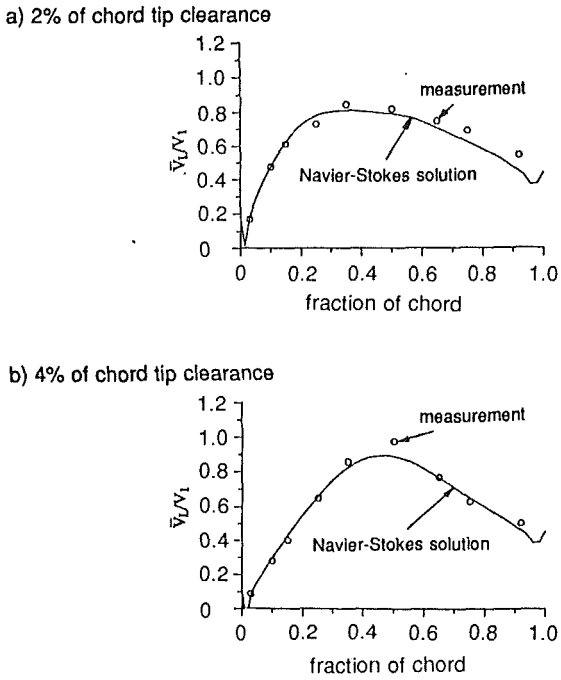

Fig. 10 Chordwise distribution of tip leakage flow averaged across the tip gap height

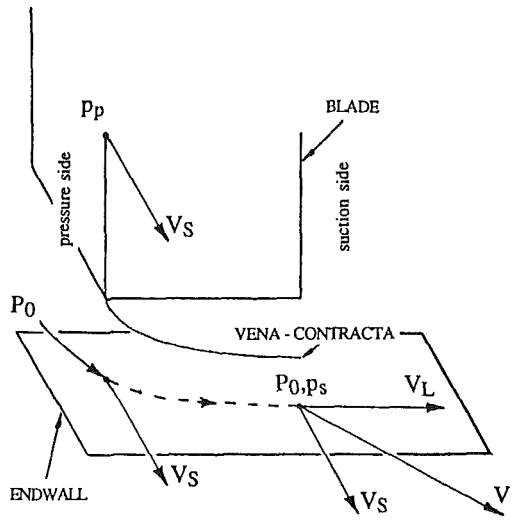

Fig. 11 The ideal flow model of Rains

nondimensional stagnation pressure loss relative to the inlet free stream, the leakage velocity nondimensionalized by the inlet velocity of the free stream, and the flow direction measured relative to the axial direction. Figure 9 shows mean absolute velocity vectors processed from the measurements with the vectors drawn from the position of the probe head used to make a measurement. The calculated trajectory of the leakage flow leaving the tip gap is also shown in Fig. 9. For present purposes the leakage velocity is defined as that component normal to the blade suction surface at the exit of the tip gap. (It is more conventional to follow Rains, 1954, and use the camberline as the reference for tip leakage flow, but since the blades are thin the choice is somewhat academic.)

With both 2 percent and 4 percent tip clearance the nature of the leakage flow was different on either side of the position of minimum pressure measured on the endwall. The difference is marked by the appearance of a distinct jet of fluid, which first emerges near the minimum pressure location and which is apparent at all the downstream measurement locations. The jet is evident in the measurements of total pressure at both 49 percent chord and 63 percent chord in Fig. 8, which show a core of very low loss fluid, bounded on the bottom by the endwall and on the top by a free shear layer at about 75 percent of the tip gap height. The flow direction remains almost constant in the core but changes by as much as 50 deg over the thickness of the shear layer (which is less than 13 percent of the tip gap height). As will be described in a future paper, the intense shearing that occurs across this thin layer between two high-speed streams of significantly different direction is the principal mechanism of the high loss associated with tip leakage flow in the cascade.

To condense the measurements of leakage flow into a more manageable form, the area-average leakage velocity, V_L, was calculated at each traverse location. This is shown in Fig. 10 plotted versus the chordwise location of the measurement for both 2 percent and 4 percent clearance. The numerical predictions of the tip leakage flow were also averaged across the blade tip and these too are presented in Fig. 10. The code predicts both the magnitude and chordwise distribution of the flow across the tip very well indeed and is sensitive to the changes in the distribution that occur when the clearance is increased.

Discussion

To understand the basic mechanisms of tip leakage it is helpful to consider a simple model owing much to Rains (1954).

A Simple Model for Tip Clearance Flow. The results in Fig. 8 show that the majority of the leakage flow with 4 percent of chord tip clearance is contained in a jet bounded by a very clearly defined free shear layer. As such the flow appears very different from the fully mixed-out flow observed by Moore and Tilton (1988) in a turbine cascade. The fact that very little mixing has taken place within the tip gap is clear from the measurement of almost zero loss of total pressure for the bulk of the flow leaving the tip gap between 49 percent chord and the trailing edge. (A similar result was obtained at 2 percent of chord clearance although this is not presented here.) The reason for less mixing across the blade tip in a compressor cascade is attributed to the much lower ratio of blade thickness to tip gap height: Measured perpendicular to the camberline the ratio in the present cascade is at most 2.5 with 2 percent of chord tip clearance, compared with a ratio of 7 in the results shown by Moore and Tilton. The observations of the flow in square-edged orifices by Ward-Smith (1971) suggest that the thickness-to-clearance ratio should characterize mixing and reattachment across a blade tip. It is important to make clear that this ratio is generally lower for compressors than for turbines because the thickness-to-chord ratio of the blades tends to be less while the running clearance as a proportion of chord is much the same.

The fact that there is negligible mixing across the blade tip causes the flow in the gap to resemble the ideal model proposed by Rains (1954) based on the solution for the potential flow into a sharp-edged orifice. Except for the stipulation that the flow separate from the corner at the entry to the tip gap, viscosity does not play a part in the model and the flow remains unattached, bounded by a free streamline along which the pressure is constant. Assuming that the contraction across the tip may be represented by a discharge coefficient (the theoretical value for a two-dimensional flow in a plane normal to the camberline and the endwall being 0.61), Rains proposed that incompressible tip leakage flow could be calculated by the simple application of the Bernoulli equation for a given pressure difference across the blade tip. The present measurements provide an opportunity to examine Rains' method and, in turn, use it to understand the mechanism controlling the flow.

A schematic diagram of the Rains' model is given in Fig. 11. It can be seen in this diagram that streamline curvature will tend to zero toward the exit of the tip gap, with the emerging jet nearly parallel to the endwall. Consequently the static pressure should be constant across the jet and, in the ideal case, so should the velocity. The absolute velocity of the leakage jet where it leaves the tip gap is therefore a function of its total pressure and the local static pressure on the suction side of the tip, viz.:

$$V = \sqrt{\frac{2\cdot(P_0 - p_s)}{\rho}} \tag{3}$$

Rains assumed that the leakage flow follows a trajectory across the blade tip such that the streamwise momentum possessed by the flow on the pressure side before it is drawn into the clearance gap is conserved. In the simple calculations described here this assumption has been retained.

As the flow accelerates into the tip gap the static pressure on the pressure side reduces toward the blade tip; this is readily shown by a solution of the two-dimensional potential flow in a plane normal to the endwall and the primary flow. The streamwise velocity of the fluid entering the tip gap cannot therefore be inferred from pressure measured *close* to the blade tip. Instead the static pressure on the pressure side of the blade outside the potential field of the inflow is a more reliable

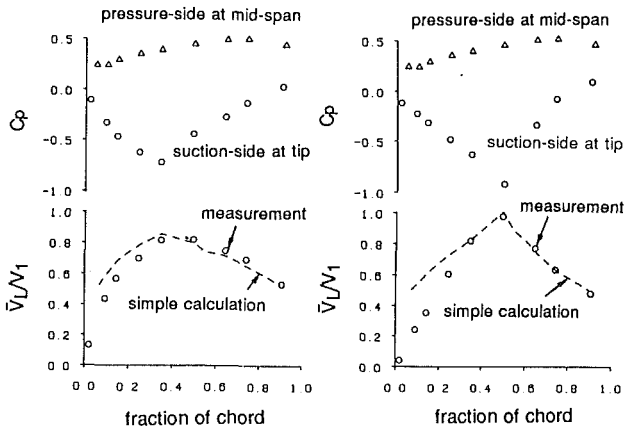

a) 2% of chord tip clearance

b) 4% of chord tip clearance

Fig. 12 Simple calculation of tip leakage flow

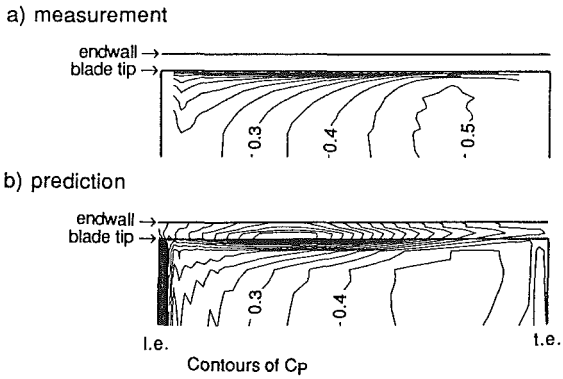

Fig. 13 Blade surface static pressure on pressure side near entry to tip gap with 4 percent of chord tip clearance

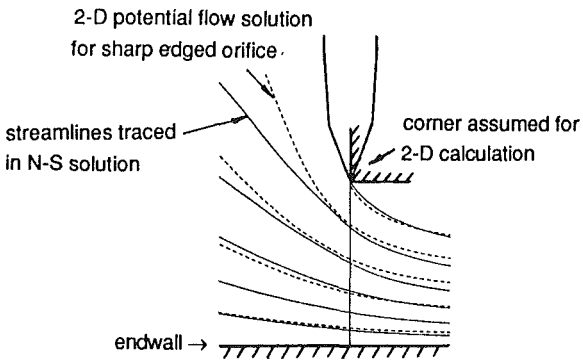

Fig. 14 Prediction of streamlines across blade tip at 97 percent of chord with 4 percent of chord tip clearance

indicator of the streamwise velocity. For present purposes the pressure is assumed to be the same as the midspan static pressure, although this is not valid near the leading edge as discussed below. The streamwise velocity entering the clearance gap at a particular chordwise location is now also obtained from the Bernoulli equation (see Fig. 9):

$$V_s = \sqrt{\frac{2\cdot(P_0 - p_p)}{\rho}} \tag{4}$$

where p_p is the static pressure at midspan on the pressure surface at the same location.

Using equations (3) and (4), an expression for leakage velocity normal to the *camberline* is obtained:

$$\frac{V_L}{V_1} = \sqrt{C_{Pp} - C_{Ps}} \tag{5}$$

The present calculation has been adjusted to give V_L as the component of velocity normal to the *suction surface* to be consistent with the presentation of the measurements.

Rains developed his method to account for resistance due to friction acting on the flow over the blade tip by incorporating a total pressure loss within the clearance space. The present measurements show that loss in the clearance gap itself is not significant and it has therefore been excluded from the calculation. A similar observation was made by Booth et al. (1981) who found that viscous effects at normal levels of clearance could be accounted for instead by small changes in the discharge coefficient.

The discharge coefficient, C_D, is used to obtain a value for the average flow rate across the tip from a prediction of actual leakage velocity according to the definition

$$\bar{V}_L = C_D \cdot V_L \tag{6}$$

A value of C_D other than the theoretical value of 0.61, which is derived from the two-dimensional analysis of the clearance flow, is essentially an empirical input to the calculation. In the present case a coefficient of 0.8 was chosen as it gave the "best fit" with experimental results. The same value was imposed at *all* chordwise locations for both 2 percent and 4 percent clearance.

The average tip leakage flow, $\bar{V}_L$, was calculated by the above method for tip clearances of 2 percent and 4 percent of chord using pressures measured in the cascade. The results are presented in Fig. 12 where they are compared directly with measured values. The upper diagram in each case shows the pressure distribution used for the calculation; it is a combination of the pressure at midspan on the pressure side (which was the same irrespective of the tip clearance) and the average static pressure measured by the two-hole probe across the exit of the tip gap on the suction side. The general level of agreement between the predictions of average leakage flow ($\bar{V}_L/V_1$) by the simple method and the measurements is good, especially over the rear 70 percent of the blade. In particular the change in the chordwise distribution of the flow across the tip that occurs with alteration of clearance is correctly indicated by the calculation.

Toward the leading edge there is a tendency for the simple method to overpredict the leakage flow, which can be seen in Fig. 12. The explanation for the discrepancy lies in the assumption of conservation of streamwise momentum across the blade tip. This is a good approximation as long as the gradient of pressure normal to the camberline is large compared to that along the blade, as Rains (1954) identified. Such a condition generally prevails downstream of the minimum pressure contour on the endwall (see Figs. 4*b* and *c*). In Fig. 13 the predicted static pressure near the tip with 4 percent clearance, obtained with the Navier–Stokes code, is compared with the corresponding measurements. Near the leading edge there is a substantial streamwise pressure gradient, comparable in magnitude to that across the tip, so that here the flow entering the tip gap experiences an appreciable acceleration in the streamwise direction. The simple model assumes that all the acceleration is produced by the pressure difference across the gap perpendicular to the camberline and therefore overestimates the flow in this direction.

The simple calculations show that, according to equation (5), it is the pressure difference across the blade tip that is the primary influence on the leakage flow. However, the pressure on the pressure side is held constant for the two cases examined and it is only the pressure on the suction side near the tip that changes with tip clearance. Therefore it is the latter that in practice controls the chordwise distribution of tip leakage flow.

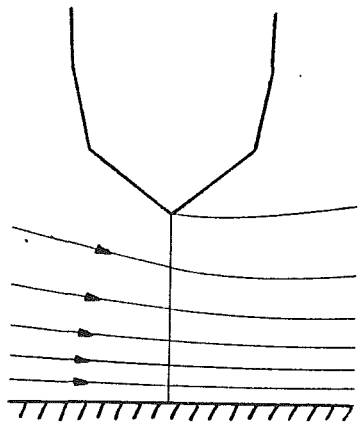

Fig. 15 Prediction of streamlines across blade tip at 14 percent chord with 4 percent of chord tip clearance

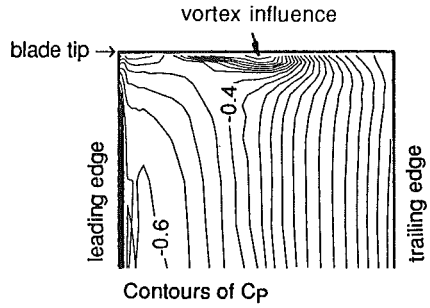

Fig. 16 Suction surface pressure distribution with 4 percent of chord tip clearance

Modeling of the Tip in the Navier–Stokes Code. The present Navier–Stokes code uses a very crude representation of the blade tip: The tip is assumed to be round so that a single point defines the tip gap height (see Fig. 3). As it stands the model of the tip does not attempt to resolve the flow in the clearance space and therefore precludes blade thickness as an important parameter in the calculation. Nevertheless the code demonstrates good overall agreement with the measurements of tip leakage flow (see, for instance, Fig. 10). This clearly suggests that tip leakage flow in the present cascade is insensitive to the tip geometry. Furthermore, since the prediction of the changes to the flowfield with tip clearance is satisfactory with an unsophisticated turbulence model, shear stresses can only play a small part in determining the flow.

When the majority of the clearance flow remains unattached across the blade tip, as in the present cascade with tip clearances greater than about 2 percent of chord, the leakage flow is in fact not influenced by blade thickness. To illustrate this point Fig. 14 shows streamlines traced across the tip at 93 percent chord in the Navier–Stokes solution for 4 percent tip clearance. Superimposed on this is the two-dimensional potential flow solution at the same clearance for comparison. It is evident that the flow approximates quite well that anticipated for a square-edged geometry without reattachment and therefore the error caused by rounding the blade tip to a single point in the computation mesh is not very large. Nearer the leading edge, for instance at 14 percent chord as shown in Fig. 13, three-dimensional calculation predicts the contraction of streamtubes across the tip to be much less.

The successful calculation of tip clearance effects by the Navier–Stokes code is determined by the prediction of the static pressure field, which is shown in Figs. 4 and 15 to be quite good. It would appear that the prediction of the static pressure field is relatively straightforward because viscous effects within the tip gap are of little significance. Instead tip leakage flow itself is responsible for large perturbations, which dominate

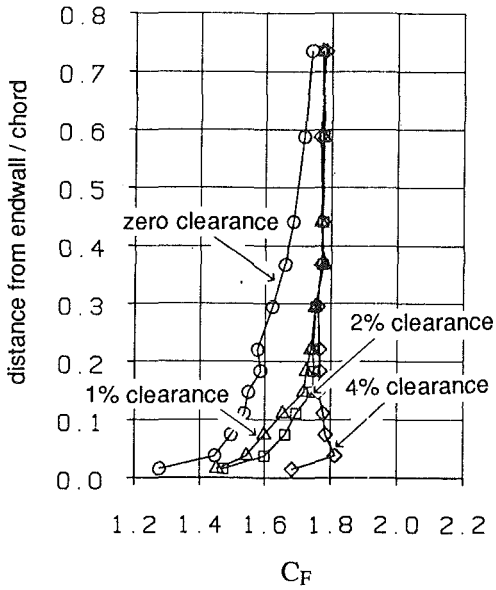

Fig. 17 Spanwise distribution of tangential blade force over a range of tip clearance

the endwall flowfield. The effects are of a scale comparable to the blade pitch and as such can be captured by a relatively coarse computation mesh.

Tip Leakage Vortex. It was not clear in the present experimental investigation whether the establishment of a leakage vortex was an inevitable consequence of tip clearance. With tip clearances less than 1 percent of chord, crude flow visualization with a wool tuft could provide no clear evidence of a vortex. With clearances upward of 2 percent of chord, a vortex could be traced to near the blade tip, which caused increasingly greater perturbation to the flowfield the greater the clearance.

The distribution of pressure near the blade tip is influenced by both the position and the strength of the leakage vortex. The blade pressure distribution for a tip clearance equal to 4 percent of chord is shown in Fig. 7, and it can be seen that the pressure distribution near the tip was affected to such an extent by the presence of a vortex that on the suction surface it hardly resembles the distribution at midspan. The influence of the vortex on blade pressure is also demonstrated by the suction-side contours shown in Fig. 16.

By producing lower pressure on the suction surface the vortex increases the local clearance volume flow. The leakage flow serves as a blockage to the primary flow in the passage and the resulting interaction as the primary flow is diverted causes pressure to rise near the leading edge. As a consequence the vortex tends to move further downstream as the tip clearance is increased, causing the minimum pressure near the blade tip to do likewise. The changes are large and it is not possible to consider the effects as simply additive, as they would be for small amplitude linear perturbations. Nevertheless it is demonstrated with the prediction of endwall pressures that the nonlinear Navier-Stokes solver is quite able to predict these effects.

Blade Force. Figure 17 shows the spanwise distribution of tangential blade force coefficient, C_F, obtained by integrating the pressure measurements over the blade surface. It can be seen that the blade force near the endwall in the present cascade tends to increase with tip clearance so that, even with a clearance of 4 percent of chord, the loading near the tip remains similar to that at midspan. Smith (1970) showed that the loss in blade force in the endwall regions, expressed as the force defect thickness, is small and is usually comparable in magnitude to the tip clearance. In the results of Smith, and of Hunter and Cumpsty (1984), there was considerable scatter in the tangential blade force defect thickness. Changes in position and strength of the clearance vortex may well be important in causing this scatter.

Relative Motion. The relative motion between rotor tips and the endwall introduces important effects (Hunter and Cumpsty, 1984; Inoue and Kuroumaru, 1989). There are two principal differences from the flow in cascades, both of which are well documented. Firstly the flow close to the endwall will be highly skewed relative to the free end of a rotor (or stator) blade, giving rise to a spanwise variation of incidence. The blade camber at rotor tips is normally small and therefore conventional secondary flow (produced by turning the flow) is generally less than that of the inlet skewing. This causes the high loss, low axial velocity fluid to collect near the pressure surface whereas in conventional cascade tests it collects near the suction surface. Secondly the flow in the endwall boundary layer possesses high relative velocity (and therefore also high relative total pressure and temperature). Some of the features of the present flowfield, for instance the effects of corner separation without tip clearance and the trajectory of the leakage vortex, may well differ in a machine, particularly in a rotor. Nevertheless the factors influencing leakage flow remain the same and it is within the capability of the present Navier-Stokes method to resolve tip leakage flow in a compressor blade row with a comparable level of agreement.

Conclusions

1 Measurements of tip leakage flow in a compressor cascade show that with a tip clearance typical of that in a machine the clearance flow separates from the blade tip and does not reattach along the majority of the chord.

2 Simple calculations based on Rains' method show that the magnitude and chordwise distribution of the tip leakage flow depend on the static pressure field near the end of the blade. Although the suction surface pressure changes with tip clearance, the pressure distribution outside the endwall boundary layer remains the primary aerodynamic input necessary to predict the overall magnitude of the flow.

3 A three-dimensional Navier-Stokes solver has shown very satisfactory predictions of many aspects of the tip clearance flow, including the static pressure field and the magnitude of the clearance flow rate along the entire chord. Since the computation mesh is relatively coarse, especially near the tip, and the turbulence modeling is unsophisticated, this shows that the tip leakage flow is controlled by a primarily inviscid mechanism.

4 The tip clearance vortex increases in size and strength as the clearance is increased. The tip clearance vortex is able substantially to alter the static pressure field near the tip on the suction side, moving the minimum pressure back along the chord as the clearance is increased. The position of the vortex relative to the suction surface is very important in determining the pressure distribution near the blade tip and the blade force.

5 Most of the clearance flow experiences very little loss within the clearance gap such that when the leakage jet emerges on the suction side its velocity is similar in magnitude to the local primary flow. Very high loss is produced in a thin layer separating the two high-speed flows near the exit of the tip gap where intense shearing is caused by the difference in flow direction.

Acknowledgments

The authors would like to thank Dr. W. N. Dawes for the use of his code. The authors are grateful for the assistance of the technical staff of the Whittle Laboratory, particularly Mr. P. Hunt for making the probes. The work was supported by

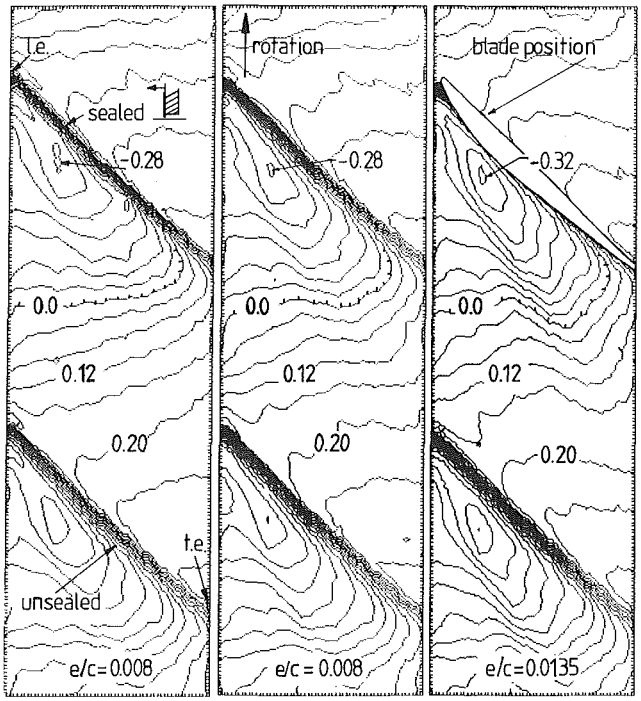

Fig. 18 Multistage rotor case wall pressure (C_p) distributions at tip clearances of 0 (sealed), 0.8, and 1.35 percent of chord showing a distinct low pressure region lying off the suction surface of the blade

Rolls-Royce plc. and the permission to publish the results is greatly appreciated.

References

Baldwin, B., and Lomax, H., 1978, "Thin Layer Approximation and Algebraic Model for Separated Turbulent Flows," AIAA Paper No. 78-257.

Dawes, W. N., 1987, "A Numerical Analysis of the Three-Dimensional Viscous Flow in a Transonic Compressor Rotor and Comparison With Experiment," ASME JOURNAL OF TURBOMACHINERY, Vol. 109, No. 1, pp. 83–90.

Freeman, C., 1985, "Effect of Tip Clearance on Compressor Stability and Engine Performance," *Tip Clearance Effects in Axial Turbomachines*, Von Karman Institute lecture series.

Hunter, I. H., and Cumpsty, N. A., 1984, "Casing Wall Boundary Layer Development Through an Isolated Compressor Rotor," ASME *Journal of Engineering for Gas Turbines and Power*, Vol. 106, No. 3, pp. 561–569.

Inoue, M., and Kuroumaru, M., 1989, "Structure of Tip Clearance Flow in an Isolated Axial Compressor Rotor," ASME JOURNAL OF TURBOMACHINERY, Vol. 111, pp. 250–256.

Moore, J., and Tilton, J. S., 1988, "Tip Leakage Flow in a Linear Turbine Cascade," ASME JOURNAL OF TURBOMACHINERY, Vol. 110, pp. 18–26.

Rains, D. A., 1954, "Tip Clearance Flows in Axial Flow Compressors and Pumps," California Institute of Technology, Hydrodynamics and Mechanical Engineering Laboratories, Report No. 5.

Smith, L. H., 1970, "Casing Boundary Layers in Multi-stage Axial Flow Compressors," *Brown Boveri: Flow Research in Blading*, L. S. Dzung, ed., Elsevier, Amsterdam.

Ward-Smith, A. J., 1971, *Pressure Losses in Ducted Flow*, Butterworths, London.